ELSEVIER

Journal of Alloys and Compounds 356–357 (2003) 442–446

Journal of ALLOYS AND COMPOUNDS

www.elsevier.com/locate/jallcom

Hydrogen absorption properties of topologically close-packed phases of the Nb–Ni–Al system

J.-M. Joubert*, C. Pommier, E. Leroy, A. Percheron-Guégan

Laboratoire de Chimie Métallurgique des Terres Rares, ISCSA, CNRS, 2–8 rue H. Dunant, 94320 Thiais Cedex, France

Received 14 July 2002; accepted 25 October 2002

Abstract

The ternary Nb–Ni–Al system presents four different topologically close-packed structures (in addition to a *C*14 phase), among which one is purely ternary (M phase) and one extends significantly in the ternary field (μ phase). Structural refinements from X-ray diffraction data for two of those phases (*A*15 Nb–Al, σ Nb–Al) are presented with a special emphasis on the structural order. Hydrogenation properties are characterized for the four phases, as a function of Nb and Al compositions for the μ phase, and are tentatively rationalized.

Keywords: Intermetallics; Hydrogen storage materials; Gas–solid reactions; Crystal structure and symmetry; X-Ray diffraction

1. Introduction

Topologically close-packed phases, also called Frank-Kasper phases, represent a large class of intermetallic compounds formed among transition metals. Their main characteristics are the exclusive presence of tetrahedral interstices and, as a consequence, the exclusive presence of Frank-Kasper coordination polyhedra. They present several features which make them attractive for studying their hydrogenation properties, among which is the possibility to be formed with elements having a strong affinity for hydrogen (so-called A-type elements: Zr, Nb, V, etc.) and the presence of tetrahedral sites in which hydrogen may locate. In addition, the existence of wide homogeneity ranges in binary or higher order systems may allow to adapt the hydrogenation properties. With the major exception of Laves phases, topologically close-packed phases have not been extensively studied as regards their hydrogenation properties. In a recent paper [1], we have reported for the first time hydrogenation properties for σ and μ phases and for *A*15 V–Ni phase. The ternary Nb–Ni–Al system [2] (Fig. 1) presents four topologically close-packed phases in addition to a ternary *C*14 phase: σ, *A*15, μ and M. All are located in the Nb-rich corner of the phase diagram and have therefore potential hydrogen absorption properties. Among them, the M phase is a purely ternary phase, not known in any other system, and the binary μ Nb–Ni phase has a large extension in the ternary field.

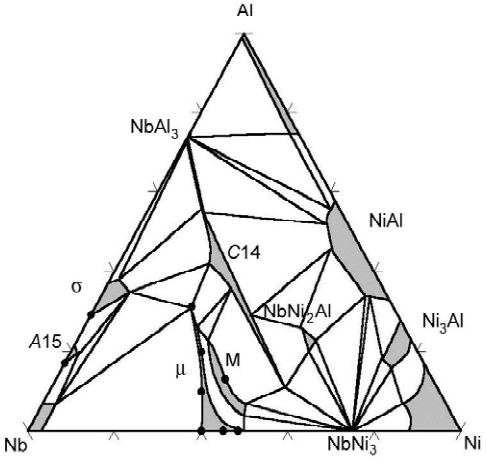

Fig. 1. Phase diagram for the Nb–Ni–Al system at 1140 °C, after Ref. [2]. Single phase fields are indicated as shaded areas. Synthesized compositions are indicated as dots.

2. Experimental

The alloys were prepared by arc melting appropriate amounts of the pure elements in an argon atmosphere.

*Corresponding author.
E-mail address: jean-marc.joubert@glvt-cnrs.fr (J.-M. Joubert).

0925-8388/02/$ – see front matter
doi:10.1016/S0925-8388(02)01238-0

Table 1
Characterization of the different alloys studied

	Phase								
	σ Nb–Al	*A*15 Nb–Al	μ Nb–Ni	μ Nb–Ni	μ Nb–Ni	μ Nb–Ni–Al	μ Nb–Ni–Al	μ Nb–Ni–Al	M Nb–Ni–Al
Nominal composition	$Nb_{71}Al_{29}$	$Nb_{83}Al_{17}$	$Nb_{51.5}Ni_{48.5}$	$Nb_{55}Ni_{45}$	$Nb_{60}Ni_{40}$	$Nb_{55}Ni_{35}Al_{10}$	$Nb_{50}Ni_{30}Al_{20}$	$Nb_{46.6}Ni_{22.1}Al_{31.3}$	$Nb_{48}Ni_{39}Al_{13}$
Structure type, Pearson symbol	CrFe, *tP*30	Cr_3Si, *cP*8	W_6Fe_7, *hR*13	W_6Fe_7, *hR*13	W_6Fe_7, *hR*13	W_6Fe_7, *hR*13	W_6Fe_7, *hR*13	W_6Fe_7, *hR*13	$Nb_{10}Ni_9Al_3$, *oP*52
Analyzed composition (at.%)	$Nb_{71(1)}Al_{29(1)}$	$Nb_{83(2)}Al_{17(2)}$	$Nb_{51.8(9)}Ni_{48.2(9)}$	$Nb_{55.3(3)}Ni_{44.7(3)}$	$Nb_{56.9(2)}Ni_{43.1(2)}$	$Nb_{54.5(6)}Ni_{35.8(6)}Al_{9.7(7)}$	$Nb_{49.7(4)}Ni_{31.9(6)}Al_{18.5(10)}$	$Nb_{47.5(4)}Ni_{23.7(12)}Al_{28.8(15)}$	$Nb_{49.2(5)}Ni_{39.4(6)}Al_{11.4(7)}$
Lattice parameters (Å)	a=9.968 c=5.165	a=5.198	a=4.915 c=26.758	a=4.946 c=26.946	a=4.959 c=26.998	a=4.966 c=27.095	a=4.984 c=27.151	a=5.015 c=27.261	a=9.358, b=4.944, c=16.291
Additional phases (wt.%)	*A*15 (8%)	σ (3%)	–	–	Nb(Ni) (9%)	Nb(Ni,Al) (6%)	–	–	–
Hydrogen capacity (H/M) (pressure)	0.51 (70 bar) reversible: 0.17 (50 bar)	0.75 (80 bar) reversible: 0.38 (80 bar)	0.10 (50 bar)	0.36 (80 bar)	0.52 (80 bar) reversible: 0.45 (100 bar)	0.52 (60 bar)	0.45 (50 bar)	0.41 (90 bar) reversible: 0.29 (100 bar)	0.36 (60 bar)

Annealing treatment was carried out under vacuum in a silica tube—the alloys were protected by a tantalum foil—for alloys in the binary Nb–Ni system and $Nb_{83}Al_{17}$ (1000 °C, 10–30 days), and $Nb_{71}Al_{29}$ (850 °C, 30 days). Ternary Nb–Ni–Al alloys were annealed at 1140 °C during 8 h in an induction furnace under argon atmosphere. The characterization of the alloys was carried out using optical microscopy and electron probe micro-analysis (EPMA). X-Ray powder diffraction data were refined using the Rietveld method, including quantitative phase analysis. Hydrogenation measurements were carried out at room temperature in a conventional Sievert's apparatus up to 100 bar. Measurements at high pressures (>25 bar) were corrected in order to take into account the non-ideality of hydrogen gas according to Ref. [3]. Pressure–composition curves were measured on the reversible capacity.

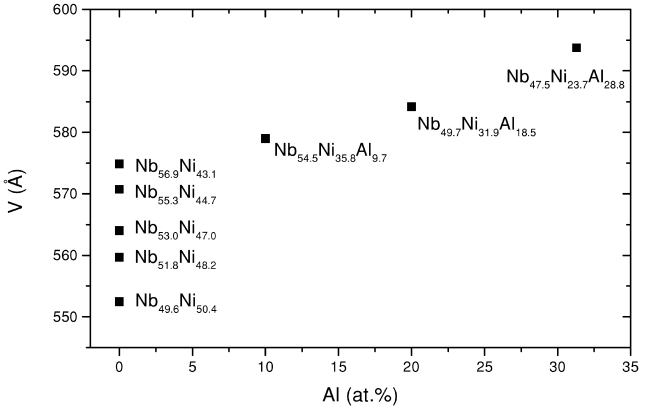

Fig. 2. Unit cell volume as a function of Al composition for binary [4] and ternary μ phases. For each compound, the composition as analyzed by EPMA is indicated.

3. Results

3.1. Metallurgy

The main results of the metallurgical and crystallographic analysis are summarized in Table 1. σ Nb–Al was synthesized at the nominal composition $Nb_{71}Al_{29}$ (a small amount of *A*15 secondary phase was observed). The structural refinement of aluminium distribution on each of the five sites of the crystal structure was constrained to the aluminium content measured by EPMA. It yields full occupancy by Nb of three of the five sites (4*f* (0.395, *x*, 0); 8*i* (0.465, 0.128, 0); 8*j* (0.181, *x*, 0.251)). Aluminium equally shares the two remaining sites with coordination number 12 (1.72(2) atom (86%) on site 2*a* (0, 0, 0); 7.02(2) atom (88%) on site 8*i* (0.740, 0.067, 0)). *A*15 Nb–Al phase was synthesized at the nominal composition $Nb_{83}Al_{17}$ with only traces of σ additional phase. The refinement of the occupancy factors on the two sites of the crystal structure indicates that the non-stoichiometry as regards the ideal composition (Nb_3Al) is accommodated by Nb substitution on aluminium site (2*a* (0, 0, 0)) in an amount of 0.46(1) atom whereas site 6*c* (1/4, 0, 1/2) is fully occupied by Nb, which yields a refined composition of $Nb_{81}Al_{19}$ in agreement with the nominal and analyzed compositions. Metallurgical and full structural characterization, including the determination of occupancy factors at each site of the structure, of μ Nb–Ni alloys has been published elsewhere [4]. All the alloys are single phase except $Nb_{60}Ni_{40}$ which presents the μ phase at its Nb-richest composition in equilibrium with Nb(Ni) terminal solid solution. Ternary μ phases have been synthesized with different aluminium contents up to 31.3 at.%. Except for $Nb_{55}Ni_{35}Al_{10}$, which presents additional Nb(Ni) terminal solid solution, all alloys are single phase. An increase in the lattice parameters as a function of aluminium composition is observed (Fig. 2). In ternary μ phases, due to the impossibility to refine more than one occupancy parameter per site, the ordering between the three atoms could not be unambiguously determined from a single diffraction data set. Finally, the ternary M phase was synthesized at the composition $Nb_{48}Ni_{39}Al_{13}$, which was obtained as a single phase. The structural refinement is in perfect agreement with the data from Ref. [5].

3.2. Hydrogenation

Hydrogen absorption by σ Nb–Al was obtained under 70 bar at room temperature. It absorbs 0.51 H/M in the first hydrogenation cycle. However, the reversible capacity obtained after desorption under vacuum at 25 °C is only 0.17 H/M, which indicates a high stability of the hydride. *A*15 Nb–Al also absorbs a capacity of 0.75 H/M at room temperature. After desorption at 140 °C under vacuum, only 50% of the capacity is recovered, which indicates again a high stability of the hydride. The hydrogenation characteristics already presented in Ref. [1] for the μ phase at the composition $Nb_{51.5}Ni_{48.5}$ could be completed as a function of Nb composition in the binary homogeneity range. Each sample absorbs at room temperature and the corresponding pressure–composition absorption curves are plotted in Fig. 3. The same behaviour was observed for ternary μ phases with aluminium and for the M phase, the pressure–composition curves are plotted in Fig. 4.

4. Discussion

4.1. Metallurgy

The crystal structures and lattice parameters are in perfect agreement with the data in the literature concerning the binary Nb–Al system [6]. Concerning the binary Nb–Ni system, it was already stated [4] that the μ phase extends more towards Nb-rich compositions than previously reported [7]. In the ternary Nb–Ni–Al diagram, the

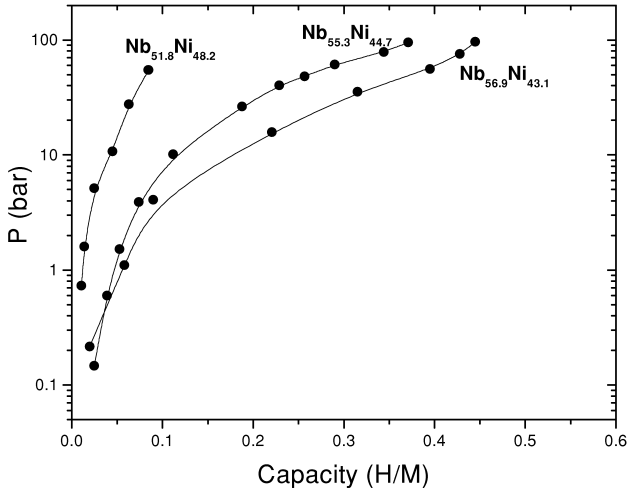

Fig. 3. Absorption pressure–composition curves for binary μ Nb–Ni phases, at 25 °C.

agreement is quite good with the reported extension of the μ phase in the ternary field [2]. The full crystal structure of both σ and *A*15 binary phases could be refined from powder diffraction data. In both cases, in order to facilitate the hydrogenation behaviour, the phases were synthesized at their maximum Nb content. The accommodation of the excess Nb atoms as regards the stoichiometric compositions (Nb_2Al and Nb_3Al) is achieved in both cases by substitution of Nb on Al sites. Contrary to what happens in numerous compounds, e.g. *A*15 V_3Pd [8] and σ Cr–Fe [9] for which the two elements may mix on each site of the crystal structure, the structures are ordered with respect to the occupancy of the Nb sites. For the σ phase, this result is in agreement with the model proposed in Ref. [10] for the stoichiometric composition from single crystal diffraction, and disagrees with the model proposed in Ref. [11] which predicts a fully disordered structure from the observation of lattice parameter changes with composition. For the *A*15 phase this result is in agreement with Ref. [12]. It is worth noting that despite the close atomic radii of Nb (R=1.46 Å) and Al (R=1.43 Å), strong ordering occurs, revealing that differences of electronic properties is the key parameter. In contrast, and as studied in detail in Ref. [4], such an order is not observed for the μ phase in the binary Nb–Ni system, since, depending on the composition, three to five among the five sites of the structure are found to be shared by the two elements.

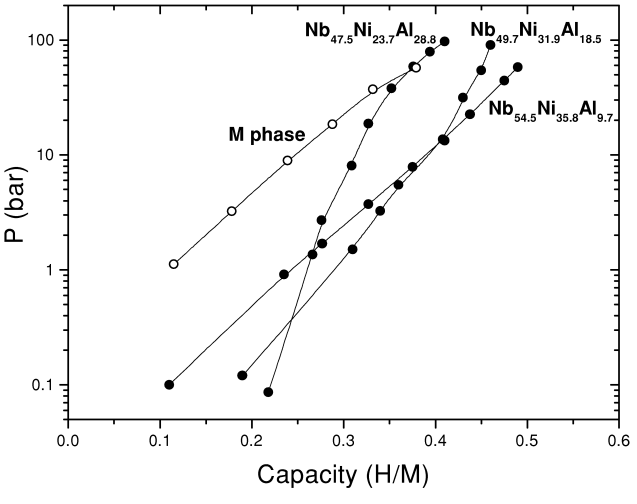

Fig. 4. Absorption pressure–composition curves for M phase and ternary μ Nb–Ni–Al phases, at 25 °C. For comparison, absorption capacity of $Nb_{47.5}Ni_{23.7}Al_{28.8}$ has been corrected to match the first cycle absorption capacity.

4.2. Hydrogenation

After σ V–Ni [1], σ Nb–Al is, as far as we know, the second σ phase reported to absorb hydrogen, with a very close absorption capacity (0.51 H/M vs. 0.46 H/M) but a higher hydride stability since it could not be desorbed completely under vacuum at room temperature. The capacity measured for *A*15 Nb–Al (0.75 H/M) is slightly higher than that obtained by Andersson et al. [12] (0.63 H/M). However, our slightly Nb-richer composition (83 at.% Nb vs. 79 at.%), could explain this small difference. It is interesting to see that the capacity measured is again of the same order as that measured for *A*15 V–Ni (0.85 H/M) [1]. The stability is, again, larger since the Nb–Al phase has been reported to release hydrogen only at 550 °C [13]. The comparison of the absorption properties of those two phases in two different systems allows to conclude that the capacity is more driven by the structural properties, e.g. the number of available sites as we will see hereunder, while the stability is more dependent on the nature and hydrogen affinity of the elements constituting the compound. The M phase in the ternary Nb–Ni–Al system is the only representative of this structure type. It is reported here, for the first time, to reversibly absorb hydrogen. The hydrogen capacity of binary μ phases is found to increase spectacularly as a function of Nb content. The substitution by aluminium yields, in a first step, a further increase in the reversible capacity, probably due to the effect of lowering absorption pressures induced by cell volume increase. However aluminium is known, in hydride systems, to decrease the capacity (e.g. in $LaNi_5$ substituted compounds [14] or among the various intermetallic phases of the Zr–Al system [15]). In addition, due to the peculiar shape of the ternary extension of the μ phase, the Nb content had to be reduced in Al-rich alloys to obtain single phase samples. These two latter parameters have the consequence, in a second step, to contradict the capacity increase provided by the lowering of absorption pressures, resulting in a stabilization or small decrease in the capacity.

The capacities observed can be tentatively rationalized among the different topologically close-packed structures investigated if one considers that: (i) only the A_4-type tetrahedral sites are occupied due to their strong affinity for

hydrogen, that (ii) no tetrahedron sharing a common face can be occupied simultaneously (to agree with the 2.1 Å rule [16,17]) and that (iii) the calculation is done with the ideal fully ordered crystal structures. Those calculations yield the following theoretical maximum capacities: 0.75 H/M for *A*15, 0.47 H/M for σ, 0.23 H/M for M and 0.23 H/M for μ phases, which are in a fair agreement with the measured capacity. Among the hydride phases investigated, only one structure has been determined: *A*15 Nb–Al [12]. In this study, it is shown that not only A_4 but also A_3B sites are occupied, but as Nb replaces Al on its sites, it is concluded that only tetrahedra composed of four Nb atoms are occupied. In the case of the μ phase, the strong disorder which exists, and the creation of new Nb_4 sites as Nb replaces Ni on its sites could be responsible for the spectacular increase in the storage capacity.

References

[1] J.-M. Joubert, A. Percheron-Guégan, J. Alloys Comp. 317–318 (2001) 71–76.
[2] N. Saunders, Aluminium–niobium–nickel, in: G. Petzow, G. Effenberg (Eds.), Ternary Alloys, MSI, VCH, 1993, pp. 348–357.
[3] H. Hemmes, A. Driessen, R. Griessen, J. Phys. C Solid State Phys. 19 (1986) 3571–3585.
[4] J.-M. Joubert, Y. Feutelais, Calphad, in press.
[5] C.B. Shoemaker, D.P. Shoemaker, Acta Crystallogr. 23 (1967) 231–238.
[6] J.-L. Jorda, R. Flükiger, J. Muller, J. Less-Common Met. 75 (1980) 227–239.
[7] T.B. Massalski, Binary Alloy Phase Diagrams, 2nd Edition, ASM International, Materials Park, OH, 1990.
[8] E.C. Van Reuth, R.M. Waterstrat, Acta Crystallogr. B24 (1968) 186–196.
[9] H.L. Yakel, Acta Crystallogr. B39 (1983) 20–28.
[10] P.J. Brown, J.B. Forsyth, Acta Crystallogr. 14 (1961) 362–364.
[11] C.G. Wilson, F.J. Spooner, J. Mater. Sci. 12 (1977) 1653–1658.
[12] Y. Andersson, T. Larsson, B. Noläng, S. Rundqvist, J. Alloys Comp. 306 (2000) 193–196.
[13] X.G. Li, K. Ohsaki, Y. Morita, M. Uda, J. Alloys Comp. 227 (1995) 141–144.
[14] H. Diaz, A. Percheron-Guégan, J.-C. Achard, C. Chatillon, J.-C. Mathieu, Int. J. Hydrogen Energy 4 (5) (1979) 445–454.
[15] N.J. Clark, E. Wu, J. Less-Common Met. 163 (1990) 227–243.
[16] D.G. Westlake, J. Less-Common Met. 90 (1983) 251–273.
[17] A.C. Switendick, Z. Phys. Chem. Neue Folge 117 (1979) 89–112.